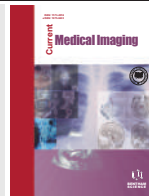


# Melanoma Skin Cancer Detection based on Image Processing



Nadia Smaoui Zghal<sup>1,\*</sup> and Nabil Derbel<sup>1</sup>

<sup>1</sup>Industrial Computer, Control and Energy Management Laboratory, National School of Engineers of Sfax, University of Sfax, Sfax, Tunisia

## ARTICLE HISTORY

Received: January 26, 2018  
Revised: August 24, 2018  
Accepted: August 28, 2018

DOI:  
10.2174/1573405614666180911120546



**Abstract: Background:** Skin cancer is one of the most common forms of cancers among humans. It can be classified as non-melanoma and melanoma. Although melanomas are less common than non-melanomas, the former is the most common cause of mortality. Therefore, it becomes necessary to develop a Computer-aided Diagnosis (CAD) aiming to detect this kind of lesion and enable the diagnosis of the disease at an early stage in order to augment the patient's survival likelihood.

**Aims:** This paper aims to develop a simple method capable of detecting and classifying skin lesions using dermoscopy images based on ABCD rules.

**Methods:** The proposed approach follows four steps. 1) The preprocessing stage consists of filtering and contrast enhancing algorithms. 2) The segmentation stage aims at detecting the lesion. 3) The feature extraction stage based on the calculation of the four parameters which are asymmetry, border irregularity, color and diameter. 4) The classification stage based on the summation of the four extracted parameters multiplied by their weights yields the total dermoscopy value (TDV); hence, the lesion is classified into benign, suspicious or malignant. The proposed approach is implemented in the MATLAB environment and the experiment is based on PH2 database containing suspicious melanoma skin cancer.

**Results and Conclusion:** Based on the experiment, the accuracy of the developed approach is 90%, which reflects its reliability.

**Keywords:** ABCD rule, multi-thresholding, skin cancer, TDV, lesion, melanoma.

## 1. INTRODUCTION

There are about 200 types of cancers which cause the messy growth of cells that invade tissues and organs. These cells can eventually spread to other tissues making them tumorous [1].

Melanoma is a type of cancer which starts, in almost all cases, in pigment cells (melanocytes) causing in general dark lesion. However, in some cases, the lesion can be pink, white or tan. Besides coloration, we can find several other characteristics of melanomas like the texture and the structures of the lesion which differentiate them from benign lesions [2].

Melanoma is considered the deadliest type of skin cancers. The American Cancer Society (ACS) estimates that about 91,270 novel cases of melanomas are diagnosed (55,150 men and 36,120 women) in 2018. In the same year, according to the ACS [3], we estimated about 9,320 fatalities (5,990 men and 3,330 women).

Mendonca *et al.* [4] mentioned that the ultraviolet light (UV) from sun exposure or other sources is the main cause

of Melanoma. About 25% of the cases develop from a mole with concerning changes including a change in color, an increase in size, and irregular edges or skin breakdown [2].

The incidence of melanoma has been increasing every year. Nevertheless, several patients could be rescued if melanoma is detected at an early stage, in which case it would be easily medicable. Recently, studies have been conducted for the early detection of melanoma [5].

Any diagnosis method requires an acquisition of a clear and illuminated image of the suspected region of the skin. The imaging instrument used for this aim is called a dermatoscope [5].

Dermoscopic images provide a more detailed view of the structures and the patterns in comparison to the normally magnified images of the skin lesions [6].

In the literature, several Computer-aided Diagnosis (CAD) systems of digital dermoscopic images have been proposed to facilitate the clinical evaluation of dermoscopic lesions. In general, a CAD system has three stages, which are: lesion detection, feature extraction, and lesion classification. For the melanoma detection process, the feature extraction is based on the ABCD rule and the classification is based on the Total Dermoscopic Value Calculation (TDV) [7].

\*Address correspondence to this author at the Industrial Computer, Control and Energy Management Laboratory, National School of Engineers of Sfax, University of Sfax, Sfax, Tunisia; Tel: 216 97489506; E-mails: nadia.smaoui@isimg.tn; nadia\_smaoui@yahoo.fr

It has been demonstrated that the ABCD method can be easily and rapidly calculated and has proven to be an effective method of providing a more objective diagnosis of Melanoma [8]. For the calculation of the ABCD rule, Asymmetry, Border, Colors and Diameter parameters are approximately estimated. Each of these parameters is then multiplied by a given weight factor in order to calculate the Total Dermatoscopy Value (TDV) and gives a clear idea about the lesion state.

The validation and the evaluation of these automatic dermoscopic image analysis systems demand a trustworthy ground truth-image database. Thus, the generation of a ground truth image database is of a critical importance, especially in the field of dermoscopy. This task must be realized by expert dermatologists. They have to manually segment and then annotate each dermoscopic image. In this process, we use the dermoscopic image database (PH2) [9] as a ground truth.

The PH2 database contains a total number of 200 melanocytic lesions, including just 40 melanomas, 80 common nevi, and 80 atypical nevi [9].

The present work aims to extract and select accurate information features in order to be used to differentiate malignant, suspicious, and benign lesions by presenting an automated cancer diagnosis based on image processing techniques.

This paper is organized as follows. Section 2 presents an overview of the previous related work. Section 3, illustrates the proposed approach to the melanoma skin cancer detection. In section 4, experimental results and analysis are presented and discussed. Finally, a brief conclusion which summarizes the results.

## 2. RELATED WORKS

In the following part, we are going to present a description of a few segmentation techniques used for the detection of skin lesion:

Glaister *et al.* segmented melanoma skin cancer images based on joint statistical texture distinctiveness. Nonetheless, one of the major drawbacks of this method is the fact that it produces a small set of data, which reduces the performance of the classification significantly [10].

In a study, authors proposed a new model for the detection of skin lesions based on region growing method for the segmentation and on SVM, KNN and fusion of SVM and KNN for the classification. Although the developed method gives good classification results, it presents some limitations, especially regarding specification of the number of clusters which requires human interference [11].

Kass *et al.* proposed a computer-aided diagnosis system which provides efficient algorithms to classify and foretell the melanoma. The proposed approach is based on enhancing the images using Contrast Limited Adaptive Histogram Equalization technique (CLAHE) and median filter. The segmentation algorithm is based on the Normalized Otsu's Segmentation (NOS) method aiming at separating the affected skin lesion from the normal skin. The classification phase is based on Neural Networks and Hybrid Adaboost-Support

Vector Machine (SVM) algorithms. The main limitation of the proposed algorithm is that it necessitates a large set of data for learning, which is not always available [12].

In our work, we will try to develop an automatic and simple method for melanoma diagnosis.

## 3. METHODS

The presented approach comprises five stages, namely: the acquisition step, the preprocessing step that is based on noise removal and contrast improvement techniques, the stage of lesion detection, feature extraction by the ABCD rule, and finally classification based on the Total Dermatoscopic Value calculation (TDV). Fig. (1) describes the proposed approach.

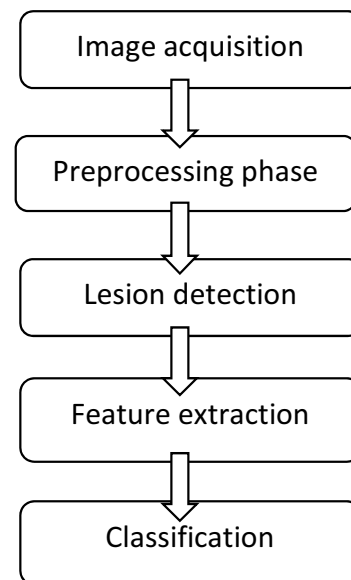


Fig. (1). Presentation of the proposed method.

### 3.1. Acquisition Step

As the early screening of melanoma significantly increases the survival rate of the patient, various noninvasive imaging techniques, like dermoscopy, have been developed to improve the detection process. Dermoscopy deploys an optical instrument together with a powerful lighting system, which enables the examination of skin lesions in a greater magnification. Thus, dermoscopic images offer a more detailed insight of the morphological structures and motives as compared to the normally magnified images of skin lesions.

In this paper, we develop a computer-aided diagnosis system of digital dermoscopic images.

The validation and the evaluation of this automatic system require a trustworthy ground truth image database. Thus, the availability of a ground truth image database is of crucial significance, especially in the dermoscopic field. This task must be realized by expert dermatologists who have to manually segment and annotate each dermoscopic image. Hence, this work is based on a dermoscopic image database (PH2). This database contains a total number of 200 melanocytic lesions, including 40 melanomas, 80 common nevi and 80 atypical nevi [9].

### 3.2. Preprocessing

The considered database is constituted by RGB images. Therefore, to treat the images, we will process each component separately as a grayscale image. Subsequently, the concatenation stage makes it possible to make colored images. The preprocessing phase is based on three steps, which are: filtering, morphological closing, and contrast enhancement.

It is important to note that for image pre-processing techniques, the choice of parameters has a major impact on the final results. Thus, better pretreatment of the images gives a better idea of the malignancy of the lesions. For that, we tried to choose the most suitable parameters for our work.

#### 3.2.1. Filtering Based on the Median Filter

In general, due to the bad affection of all manners of noise, the medical image quality is clearly degraded. This can cause a serious obstacle for image segmentation and recognition. To reduce the noise, the image must first be denoised. The median filter is an important noise reduction method. It is based on sorting all the entries in the window and then replacing the central pixel by the middle value, thus noise is reduced to a certain extent [13]. The impact of the median filter with a 5\*5 window on the original image is presented in Fig. (2a, b).

For our case, this choice of window size gives better results in the classification phase.

#### 3.2.2. Morphological Closing

Morphological operators are non-linear filters. They can be applied to both binary and grayscale images. In our work, we are interested in the grayscale morphology. The basic idea of mathematical morphology is to compare the image analyzed with a set of known geometry form called "structuring element" [14]. The morphological closing consists of a dilation followed by erosion. The dilation "extends" an image according to the shape of the structuring element. The erosion step "shrinks" the resulting image with the same structuring element [14]. The application of the morphological closing on the filtered image with a line structuring element is presented in Fig. (2c).

We can notice that the morphological closing eliminates all artifacts like the hairs that remain after filtering with the median filter.

#### 3.2.3. Contrast Enhancement

The aim of the contrast enhancement is to have better visibility of the image details without introducing unrealistic visual apparition and/or unwanted artifacts. To do that, we

are based on the imadjust function in the Matlab environment. This function maps intensity values of the image in such a way that 1% of data are saturated at high and low intensities. The effect of the adjustment operation in the image is presented in Fig. (2d).

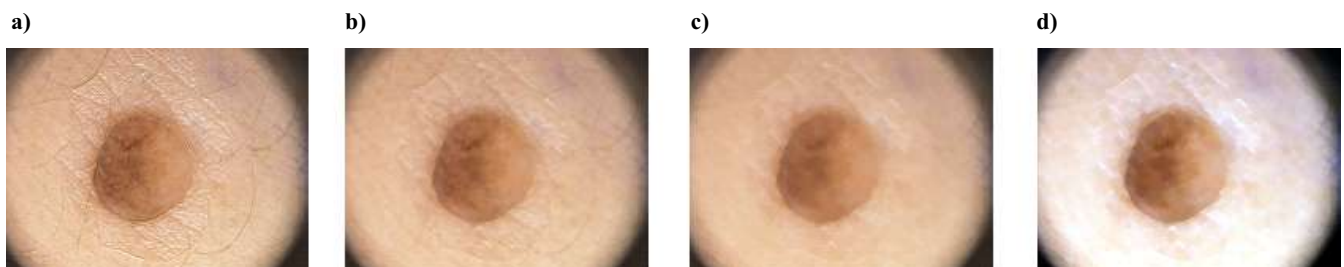
### 3.3. Black Frame Removing and Lesion Detection

After the pretreatment steps, we need to remove the black frame which is introduced during the digitization process and to detect the lesion. To achieve this goal, we must define a binary mask showing the dark parts of the image (low gray values). In general, the binarization step based on the Otsu thresholding method [15], which classifies pixels in two classes, has some limitations since both the lesion and the edges present a fairly dark gray level. To overcome this shortcoming, we use the Multi thresholding Otsu [16] which is suitable to produce multiple classes and multiple thresholds from one single image. In fact, the dermatoscopic image converted into a gray level image has essentially three parts which are the edges (the darkest part), the lesion and the skin which is the lighter part. By setting the desired number of classes to three (the algorithm needs to find two thresholds), we can get background pixels, intermediate pixels and bright pixels.

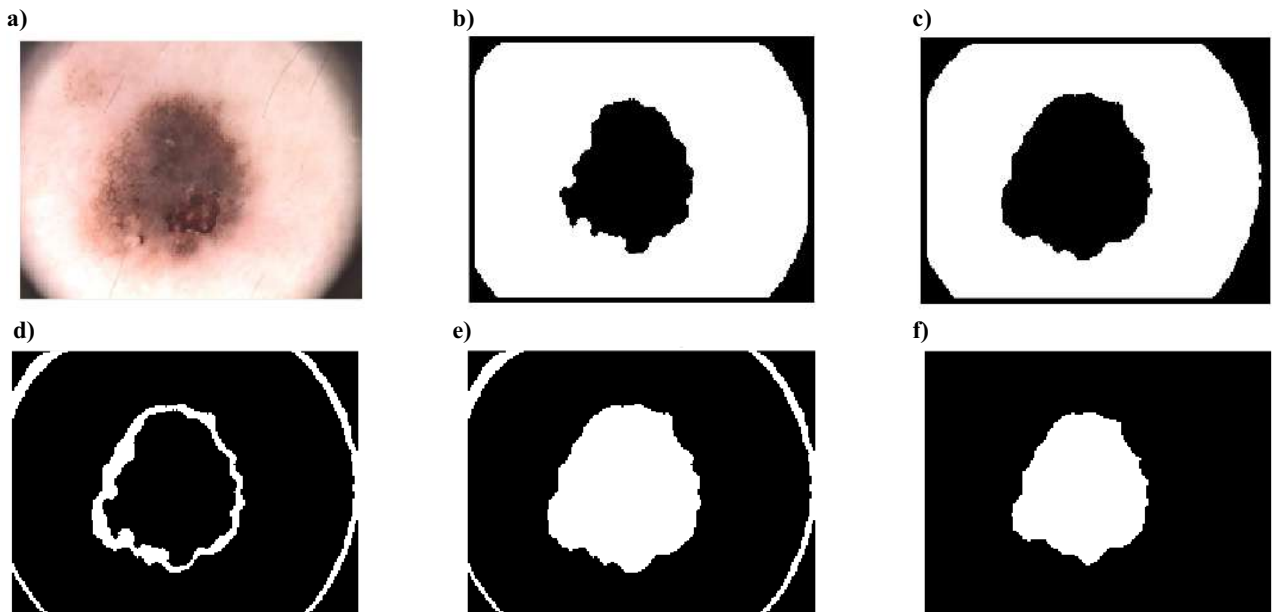
In our work, the goal is to define a mask of the original image (Fig. 3a) that considers only the lesion. For this purpose, we present two binary masks, the first is based on the first threshold found by the Multi-otsu thresholding algorithm (Fig. 3b), and the second is based on the second threshold (Fig. 3c). Thus, in the first mask, we consider the dark part of the image with the edges and in the second mask the lighter part. A simple subtraction between the two masks makes it possible to eliminate a good part of the edges and to keep the contour of the lesion as presented in Fig. (3d). Once the contour is detected, we perform the flood-fill operation [17] starting from the center pixel. The resulted mask is presented in Fig. (3e). The lesion is detected but the edges of the image still persist. It is therefore sufficient to apply a simple erosion [18] to completely eliminate the edges as shown in Fig. (3f). Finally, the mask is superimposed to the three components in order to obtain the result presented in Fig. (4). We notice that we are based on a white inclusion.

### 3.4. Feature Extraction and Classification

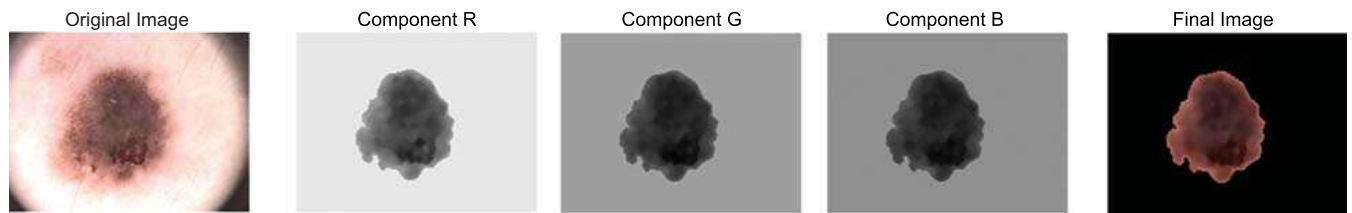
ABCD rule is one of the most popular methods for the evaluation of melanocytic lesions. This method was originally proposed in 1994 by Nachbar *et al.* [19]. Premaladha and Ravichandran [18] have proved the reliability of the ABCD



**Fig. (2).** Pre-treatment steps: (a) Original image, (b) Application of median filter, (c) Application of morphological closing, (d) Contrast enhancement. (A higher resolution / colour version of this figure is available in the electronic copy of the article).



**Fig. (3).** Definition of the mask: (a) Original image, (b) Mask1 (with the first threshold), (c) Mask2 (with the second threshold), (d) Mask2-Mask1, (e) Application of filling operator, (f) Final Mask. (A higher resolution / colour version of this figure is available in the electronic copy of the article).



**Fig. (4).** Application of the mask on the three components. (A higher resolution / colour version of this figure is available in the electronic copy of the article).

**Table 1.** Presentation of criteria of ABCD rules.

Criterion	Description	Score	Weight factor
Asymmetry	Assess not only contour, but also colors	0-2	X 1.3
Border	Abrupt ending of pigment pattern at the periphery in 0-8 segments	0-8	X 0.1
Color	Presence of up to 6 colors (white, red, light brown, dark brown, blue-gray, black)	1-6	X 0.5
Diameter	>6mm indicates the presence of melanoma	0.5-5	X 0.5

rule in a prospective study. In fact, for 172 melanocytic lesions (103 melanocytic nevi and 69 melanomas) specificity was 90.3% and sensitivity was 92.8% [8]. To calculate the ABCD score, the asymmetry (A), the border irregularity (B), the amount of colors (C), and the diameter (D) have to be evaluated semiquantitatively. The Table 1 resumes these criteria. It is important to say that the most important parameter is the asymmetry indicator. Second, consider the parameter of irregularity. After that, it will be the color parameter and finally, the diameter indicator which is the least important since the way of measuring is not always so precise.

Most of the clinicians are familiar with Asymmetry, Border, Color and Diameter (ABCD) analysis to predict and diagnose the melanoma. But Asymmetry plays a major role

and it will be one of the best indicators to confirm the presence of cancerous melanocytes.

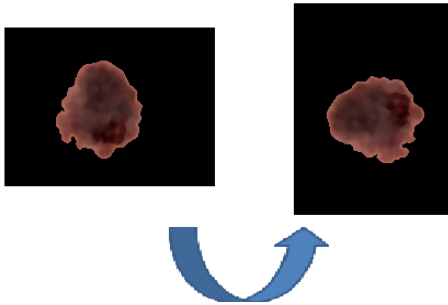
After measuring ABCD parameters, each of the criteria (A,B,C,D) has to be multiplied by a given weight factor (Table 1) in order to calculate the total dermoscopy value (TDV) as follows:

$$TDV = 1.3 * A + 0.1 * B + 0.5 * C + 0.5 * D \quad (1)$$

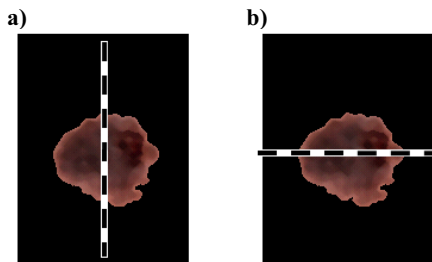
The result of TDV shows whether the lesion is benign or malignant. A TDV less than 4.75 indicates a benign lesion, a TDV between 4.8 and 5.45 indicates a suspicious lesion and a TDV larger than 5.45 indicates a malignant melanocytic lesion [19]. In the following section, we will try to compute each of the indicators A, B, C and D in order to find the TDV value.

**3.4.1. Asymmetry**

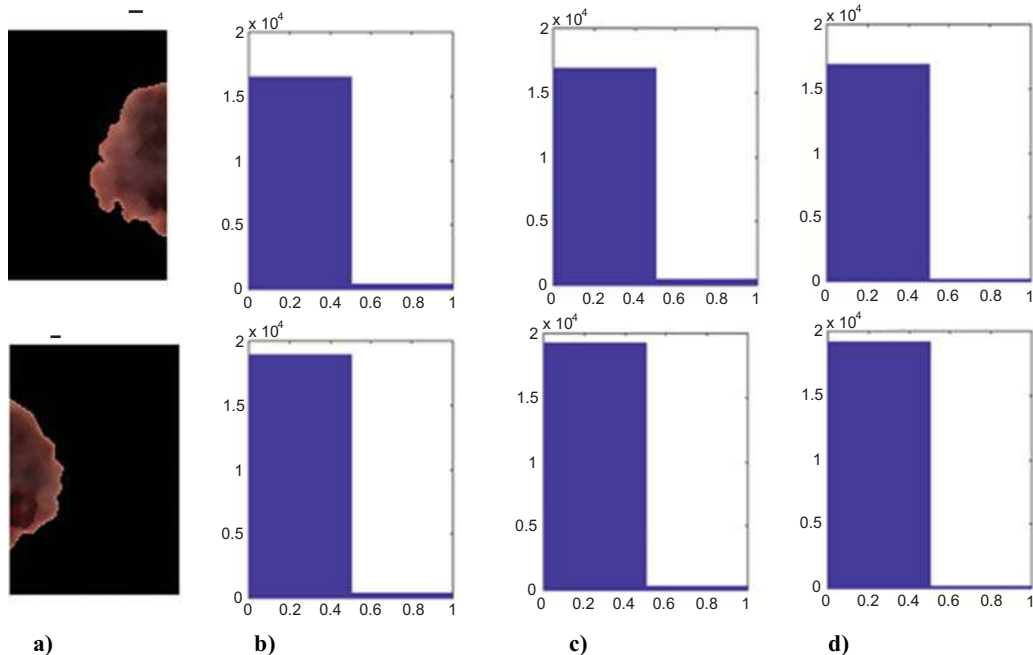
This characteristic is the major important indicator of malignancy. This parameter is considered in terms of form and color. To facilitate the task of computing the score of asymmetry, we propose to translate the lesion to the center of the image and we rotate it to align the major axis horizontally as presented in Fig. (5). Now it is simple to divide the image according to the minor axis and the major axis of the lesion (Fig. 6).



**Fig. (5).** Rotation of the lesion. (A higher resolution / colour version of this figure is available in the electronic copy of the article).



**Fig. (6).** Division of the lesion according to: (a) The major axis and (b) The minor axis. (A higher resolution / colour version of this figure is available in the electronic copy of the article).

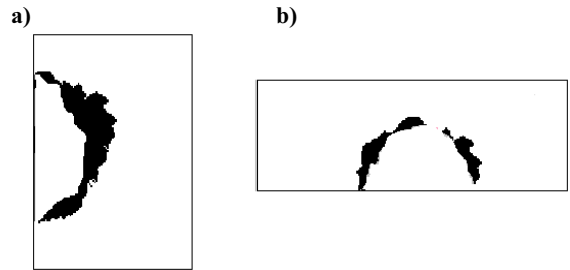


**Fig. (8).** Presentation of histograms of the 3 RGB components of each part: (a) Presentation of each part, (b) Histogram of component R, (c) Histogram of component B, (d) Histogram of component G. (A higher resolution / colour version of this figure is available in the electronic copy of the article).

To measure the asymmetry, we are based on folding the outline of the lesion according to the major axis and the minor axis. Then, we compute the non-overlapping area between the two vertical (left vs. right) and horizontal (upper vs. lower) parts. The result of the non-overlapping operation between left and right halves is presented in Fig. (7a). And the result of the non-overlapping operation between upper and down halves is presented in Fig. (7b). Hence, the asymmetry score  $\Delta A$  is calculated as follows:

$$\Delta A = \begin{cases} 0, & OVL(L,R) \leq T0 \text{ and } OVL(U,d) \leq T0 \\ 1, & OVL(L,R) \leq T0 \text{ or } OVL(U,d) \leq T0 \\ 2, & \text{otherwise} \end{cases} \quad (2)$$

Where T0 is an overlapping threshold value=5%.



**Fig. (7).** Non-overlapping Area: (a) Left-right folding, (b) Upper-lower folding. (A higher resolution / colour version of this figure is available in the electronic copy of the article).

Finally, the computation of the asymmetry in terms of form is calculated as follows:

$$A_{form} = \frac{\Delta A}{AL} \quad (3)$$

Where AL is the total area of the lesion.

To measure color asymmetry, histograms of the three RGB components of each part of the lesion have been plotted (Fig. 8). Then, histograms have been normalized. This being done by associating the 3 histograms of the components R, G and B. Then each histogram is divided by 3 as presented by the following equations:

$$hist1 = \frac{hist1}{3} \tag{4}$$

$$hist2 = \frac{hist2}{3} \tag{5}$$

Afterwards, the distance between the two normalized histograms has been calculated using the Chi-Square distance [20] presented by the following equation:

$$Acolor = Chi\_s = \sum_{i=1}^n \frac{(hist1(i)-hist2(i))^2}{hist1(i)+hist2(i)} \tag{6}$$

The Chi-square value is an expression of color variation within the image. A lesion with only a single color will have identical normalized color histograms and therefore have Chi-square=0.

Finally, the asymmetry score A is computed according to the following equation:

$$A = \frac{Aform+Acolor}{2} \tag{7}$$

### 3.4.2. Border Irregularity

In general, the edges of the benign lesions are fairly regular. Irregularity of the edge can indicate cancer propagating. To compute the Border Irregularity parameter, the lesions are divided into eight sectors as demonstrated in Fig. (9).

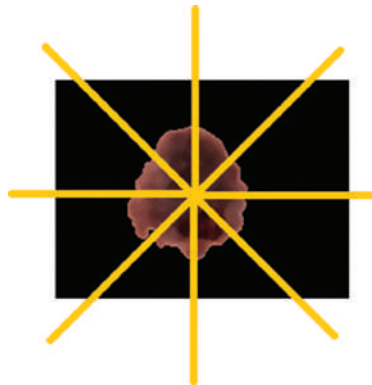


Fig. (9). Lesion divided into eight sectors for border calculation. (A higher resolution / colour version of this figure is available in the electronic copy of the article).

Table 2. RGB codes.

White	Black	Red	Light-Brown	Dark-Brown	Blue-Gray
(1,1,1)	(0,0,0)	(0.7843, 0.5882, 0.3922)	(0.7843, 0.5882, 0.3922)	(0.5882, 0.3922, 0.3922)	(0.5882, 0.4902, 0.5882)
(0.9608, 0.9608, 0.9608)	(0.0392, 0.0392, 0.0392)	(1,0.1961, 0.1961)	(0.7843, 0.3922, 0)	(0.4902, 0.2941, 0.2941)	(0.4902, 0.4902, 0.5882)
(0.9216, 0.9216, 0.9216)	(0.0784, 0.0784, 0.0784)	(0.7843, 0, 0)	(0.7843, 0.3922, 0.1961)	(0.3922, 0.1961, 0.1961)	(0.3922, 0.3922, 0.4902)
(0.8824, 0.8824, 0.8824)	(0.1176, 0.1176, 0.1176)	(0.7843, 0.1961, 0.1961)	(0.5882, 0.3922, 0.1961)	(0.3922, 0.1961, 0)	(0.3922, 0.4902, 0.5882)
(0.8431, 0.8431, 0.8431)	(0.1569, 0.1569, 0.1569)	(0.5882, 0, 0)	(0.5882, 0.3922, 0)	(0.3922, 0, 0)	(0.1961, 0.3922, 0.5882)
(0.8039, 0.8039, 0.8039)	(0.1961, 0.1961, 0.1961)	(0.5882, 0.1961, 0.1961)	(0.5882, 0.1961, 0)	(0.1961, 0, 0)	(0, 0.3922, 0.5882)

To do that, the Euclidean distance [21] is computed for each pixel of the lesion border edge (as defined by the lesion mask) as shown by the following equation:

$$Di = \sqrt{(xc - xi)^2 + (yc - yi)^2} \tag{8}$$

xi and yi are the coordinates of pixel, xc and yc are the coordinates of the center of the lesion. The sum of the distances is calculated according to the following equation:

$$Distance = \sum Di ; i = 1..n \tag{9}$$

n is the number of pixels in the edge.

Each of eight sectors is defined by the angles (0°...45°; 45°...90°; 90°...135°; 135°...180°; 180°...225°; 225°...270°; 270°...315°; 315°...360°) relative to the center point.

Once the eight sectors are defined (Fig. 9), the standard deviation for each sector is calculated using the following equation:

$$s = \left( \frac{1}{n-1} \sum_{i=1}^n (xi - \bar{x})^2 \right)^{1/2} \tag{10}$$

Where  $\bar{x} = \frac{1}{n} \sum_{i=1}^n xi$  and n is the number of elements in the sector.

Within each sector, if the standard deviation exceeds a certain threshold, the border score is 1. This threshold is fixed empirically at 30. Thus, the maximum irregular border score is 8 and the minimum is 0.

### 3.4.3. Color

To check the presence of each of the colors: white, red, light brown, dark brown, gray-blue and black, we use the approach proposed by Grammatikopoulos *et al.* [22]. For a given image showing the lesion, it is necessary to examine the presence of the six candidate colors appearance.

To do this, the distance between the examined pixel value in the lesion and each color reference is calculated. If this value is below or equal to the “pre-calculated threshold value (see below)”, then the color score is incremented by 1.

The RGB codes chosen as reference points for each color are presented in Table 2. In this table, RGB codes for colors are presented. Top rows are codes for the base colors, succeeding rows for gradually less intensive tones of the colors.

And the distance of a color reference calculated for pixels in the lesion is based on the Euclidean Distance indicated by the following equation:

$$C_{k(i,j)} = \sqrt{(r_k - r_{ij})^2 + (g_k - g_{ij})^2 + (b_k - b_{ij})^2} \quad (11)$$

$k = 1 \dots 6$  and  $(i,j)$  is the pixel's position in the lesion.

Now,  $Ck$ ;  $k = 1 \dots 6$  is calculated as follows:

$$Ck = \frac{\sum Ck(i,j)}{n} \quad (12)$$

Where  $n$  is the number of pixels in the lesion.

The existence of colors in the lesion depends on the comparison between  $Ck$  and the threshold value.

For each color, a threshold value  $T_k$  is computed as a distance between the highest and the smallest reference value. In the following equation, we present an example of the white color:

$$T_0 = \sqrt{3 * (1 - 0.8039)^2} = 0.3397 \quad (13)$$

The same method is repeated for other colors for the calculation of their threshold values. The color score is incremented by 1 if  $C_k \leq T_k$ .

**3.4.4. Diameter**

The number of pixels of the major axis length (the largest diameter) of the lesion is transferred into millimeter scale as presented by the equation (14):

$$M = \frac{\text{majoraxislength} * 25.4}{\text{dpi}} \quad (14)$$

With dpi is the dot per inch. It is equal to 96.

Then, the diameter score is calculated as follows:

$$\begin{cases} D = 0.5 & M < 2mm \\ D = 1 & M < 3mm \\ \vdots & \\ D = 4.5 & M < 10mm \\ D = 5 & otherwise \end{cases} \quad (15)$$




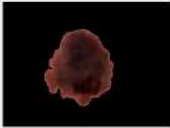








Finally, The TDV value is calculated according to equation (1).

**4. EXPERIMENTAL RESULTS AND DISCUSSION**

**4.1. Experimental Results**

The developed method is applied to the PH2 database. In Table 3, we present a random selection of segmentation and classification of results. For each image, the segmented lesion is presented with the calculated value of the TDV and the classification result. The expert opinion is also exposed to each case in order to evaluate the proposed approach.

**Table 3. Segmentation results.**

Original Image	Detected Lesion	TDS Score	Result	Expert Opinion
		(A= 1, B=2 , C=2, D=1.5 → TDS=3.25)	Benign	Benign
		(A= 0.5, B=2 , C=2, D=2 → TDS=2.85)	Benign	Benign
		(A= 0.5, B=1 , C=2, D=1.5 → TDS=2.5)	Benign	Benign
		(A= 0.5, B=1 , C=2, D=1 → TDS=2.25)	Benign	Benign
		(A= 2, B=3 , C=3, D=3 → TDS=5.9)	Malignant	Malignant
		(A= 2, B=2 , C=3, D=3.5 → TDS=6.05)	Malignant	Malignant

**Table 4. Summary of the calculated values.**

	Benign (B)	Suspicious (S)	Melanoma (M)
TP	74	64	36
FN	6	16	4
FP	11	10	8
TN	109	110	152

**Table 5. Evaluation metrics of the proposed work.**

	Class			Average (our work)	Average[22]
	B	S	M		
Sensitivity	92.5%	80%	90%	87.5%	93%
Specificity	90.8%	91.6%	95%	92.46%	85%
Accuracy	91.5%	87%	94%	90.83%	-

**4.2. Discussion**

First, the skin lesion mask is created and then it is applied to the preprocessed image to obtain the segmented image. The input image of the skin lesion is efficiently segmented for both moles as well as Melanoma as presented in Table 3. Thereafter, the ABCD rule is applied to yield for the calculation of the TDV score which gives an idea about the malignancy of the lesion (Table 3).

For the evaluation of our work, results of this research have been compared with those of [22], in terms of sensitivity, specificity and accuracy. These three metrics are presented by the following equations:

$$\text{Sensitivity} = \frac{TP}{TP+FN} \tag{16}$$

$$\text{Specificity} = \frac{TN}{TN+FP} \tag{17}$$

$$\text{Accuracy} = \frac{Tp+TN}{TP+FP+FN+TN} \tag{18}$$

With: TP=number of true positives, TN=number of true negatives, FN=number of false negatives, FP=number of false positives.

A positive result is a lesion which is classified as malignant, and a negative result is a lesion that is classified as benign.

It is to keep in mind that our research is based on PH<sup>2</sup> dataset which contains 40 melanomas, 80 common nevi and 80 atypical nevi [5]. Table 4 summarizes the calculated values of the three classes namely benign (B), Suspicious (S) and Melanoma (M) and Table 5 presents the three evaluation metrics.

From this table, it can be concluded that although the proposed approach is simpler than that developed in [22], the results found are close to those of [22] and are even better. It can, therefore, be concluded that these results are satisfactory.

From this actual output, it can be concluded that the proposed approach can be strongly used by patients and physicians to diagnose the skin cancer more precisely.

**CONCLUSION**

Melanoma is the most dangerous and the most aggressive skin cancer, its early detection is vital. To decrease the cost and increase the accuracy of the detection process, an automated melanoma detection system is needed. In this paper, we present an automatic system for the detection of pigmented skin lesions and melanoma diagnosis, based on PH2 database containing suspicious melanoma skin cancer. The developed approach consists of a preprocessing step, a segmentation step which is in turn based on multilevel thresholding algorithm, the feature extraction by the ABCD rule, and finally, the classification based on the Total Dermatoscopic Value calculation (TDV). The proposed method classifies images with a specificity of 92% and a sensitivity of 87%, which reflects its reliability.

**LIST OF ABBREVIATIONS**

- ABCD= Assymetry Border Color Diameter
- ACS = American Cancer Society
- CAD = Computer-aided Diagnosis
- TDV = Total Dermoscopy Value
- SVM = Support Vector Machine

**ETHICS APPROVAL AND CONSENT TO PARTICIPATE**

Not applicable.

**HUMAN AND ANIMAL RIGHTS**

No animals/humans were used for studies that are the basis of this research.



**CONSENT FOR PUBLICATIN**

Not applicable.

**AVAILABILITY OF DATA AND MATERIALS**

The data that support the findings of this study are available at <https://www.fc.up.pt/addi/ph2%20database.html>.

**FUNDING**

None.

**CONFLICT OF INTEREST**

The authors declare no conflict of interest, financial or otherwise.

**ACKNOWLEDGEMENTS**

Declared none.

**REFERENCES**

- [1] Soyer HP, Argenziano G, Hofmann-Wellenhof R, Zalaudek I. *Dermoscopy: The Essentials*. 2<sup>nd</sup> ed. Elsevier: Saunders 2011.
- [2] Johr RH. Dermoscopy: alternative melanocytic algorithms-the ABCD rule of dermatoscopy, Menzies scoring method, and 7-point checklist. *Clin Dermatol* 2002; 20(3): 240-7. [[http://dx.doi.org/10.1016/S0738-081X\(02\)00236-5](http://dx.doi.org/10.1016/S0738-081X(02)00236-5)] [PMID: 12074859]
- [3] American cancer Society. Key statistics for melanoma skin cancer. Available from: <https://www.cancer.org/cancer/melanoma-skin-cancer/about/key-statistics.html> accessed July 2018.
- [4] Mendonca T, Ferreira PM, Marques JS, Marcal AR, Rozeira J. PH<sup>2</sup>- a dermoscopic image database for research and benchmarking. *Conf Proc IEEE Eng Med Biol Soc* 2013; 2013: 5437-40.
- [5] Mendonca TF, Ferreira PM, *et al.* PH<sup>2</sup> - A public database for the analysis of Dermoscopic images. CRC Press 2015; pp. 419-39. [<http://dx.doi.org/10.1201/b19107-14>]
- [6] Sumithra R, Mahamad S, Guru DS. Segmentation and classification of skin lesions for disease diagnosis. *Procedia Comp Sci* 2015; 45: 76-85.
- [7] Jaworek-Korjakowska J. Novel method for border irregularity assessment in dermoscopic color images. *Comput Math Method Med* 2015; 496202:1-11. [<http://dx.doi.org/10.1155/2015/496202>]
- [8] Stolz W. ABCD rule of dermatoscopy: a new practical method for early recognition of malignant melanoma. *European J Dermatol* 1994; 4: 521-7.
- [9] ADDI Project. PH<sup>2</sup> database, Automatic Computer-Based Diagnosis System for Dermoscopy Images; 2012. Available from: <https://www.fc.up.pt/addi/ph2%20database.html> accessed July 2017.
- [10] Glaister J, Wong A, Clausi DA. Segmentation of skin lesions from digital images using joint statistical texture distinctiveness. *IEEE Trans Biomed Eng* 2014; 61(4): 1220-30. [<http://dx.doi.org/10.1109/TBME.2013.2297622>] [PMID: 24658246]
- [11] Alcón JF, Ciuhu C, Ten Kate W, *et al.* Automatic imaging system with decision support for inspection of pigmented skin lesions and melanoma diagnosis. *IEEE J Sel Top Signal Process* 2009; 3: 14-25. [<http://dx.doi.org/10.1109/JSTSP.2008.2011156>]
- [12] Kass M, Witkin A, Terzopoulos D. Snakes: active contour models. *Int J Comput Vis* 1988; 1: 321-31. [<http://dx.doi.org/10.1007/BF00133570>]
- [13] Huang T, Yang G, Tang G. A fast two-dimensional median filtering algorithm. *IEEE Trans Acoust Speech Signal Process* 1979; 27(1): 13-8. [<http://dx.doi.org/10.1109/TASSP.1979.1163188>]
- [14] Soille P. *Morphological Image Analysis*. Berlin: Springer-Verlag 1999. [<http://dx.doi.org/10.1007/978-3-662-03939-7>]
- [15] Otsu N. A threshold selection method from gray-level histograms. *IEEE Trans Syst Man Cybern* 1979; 9: 62-6. [<http://dx.doi.org/10.1109/TSMC.1979.4310076>]
- [16] Liao P-S, Chung P-C. A fast algorithm for multilevel thresholding. *J Inf Sci Eng* 2001; 17(5): 713-27.
- [17] Hassanpour H, Samadiani N, Salehi SMM. Using morphological transforms to enhance the contrast of medical images. *Egyptian J Radiol Nucl Med* 2015; 46(2): 481-9. [<http://dx.doi.org/10.1016/j.ejrm.2015.01.004>]
- [18] Premaladha J, Ravichandran KS. Novel Approaches for Diagnosing Melanoma Skin Lesions through Supervised and Deep Learning Algorithms. *J Med Syst* 2016; 40: 96. [<http://dx.doi.org/10.1007/s10916-016-0460-2>]
- [19] Nachbar F, Stolz W, Merkle T, *et al.* The ABCD rule of dermatoscopy. High prospective value in the diagnosis of doubtful melanocytic skin lesions. *J Am Acad Dermatol* 1994; 30(4): 551-9. [[http://dx.doi.org/10.1016/S0190-9622\(94\)70061-3](http://dx.doi.org/10.1016/S0190-9622(94)70061-3)] [PMID: 8157780]
- [20] Celebi ME, Stoecker WV, Moss RH. Advances in skin cancer image analysis. *Comput Med Imaging Graph* 2011; 35(2): 83-4. [<http://dx.doi.org/10.1016/j.compmedimag.2010.11.005>] [PMID: 21145206]
- [21] Westerink PH, Biemond J, Boeke DE. Subbandcoding of color images. In: Coding SI, Woods, JW, Eds. *Kluwer Academic Publishers, Inc* 1991; pp. 193-228.
- [22] Grammatikopoulos G, Hatzigaidas A, Papastergiou A, *et al.* Automated malignant melanoma detection using MATLAB. *Proceedings of the 5<sup>th</sup> WSEAS Int. Conf. on data networks, communications & computers*. Bucharest, Romania, October 16-17 2006; pp. 91-4.